International Conference on Estuaries and Coasts
November 9-11, 2003, Hangzhou, China

NEW DEVELOPMENT IN NUMERICAL SIMULATION OF THE TIDAL BORE

Cunhong PAN
Zhejiang Institute of Hydraulics and Estuary, Hangzhou, 310020,China
E-mail: panch@mail.hz.zj.cn

Bingyao LIN & Xianzhong MAO
Zhejiang Institute of Hydraulics and Estuary, Hangzhou, 310020,China

Abstract: Using Godunov-type scheme with water level-bottom topography formulation, the 2-D shallow-water equations with bottom topography can be solved. The Riemann solution of dry bed problem is applied to solve moving boundary. Based on verification of the typical shallow transcritical flows(Pan et al., 2003), the mathematical model is applied to simulate the formation, evolution and dissipation of the tidal bore on the Qiantang River. A good agreement is made between the computed and field measurements, and it also numerically replicates the phenomena of the intersecting, reflection of the tidal bores, line-type tidal bore, which leads to more understanding about the tidal bores on the Qiantang River.

Key words: The Qiantang River, Godunov scheme, Tidal bore, Numerical simulation, Moving boundary

1. INTRODUCTION

Hangzhou Bay, which is the bay of Qiantang Estuary, is a unique funnel shape bay. The Bay mouth is about 100km wide, narrowing upstream to 22 km wide at the head of the Bay, Ganpu, which is 89km away from the Bay mouth. With rapid narrowing, the tidal range is increased by up to 75% at Ganpu, and the maximum observed record is 9.0m. From Ganpu goes upstream, there is a prodigious sand bar along the river, and it leads water depth decrease, and the shallow-water effect increase, as a result, it makes tidal wave severely deform, and finally develop Qiantang Bore, which is the most spectacular one in the world.

The tidal bore is a local phenomenon and a part of tidal wave. There is complex structure within the tidal bore at the range of several times of water depth before/after the bore during a few minutes when tidal level rises suddenly (Pan et al., 1994; Wan, 1996; Lin et al., 1998). On the other hand, tidal wave period is more than 12hours, and tidal wave length is hundreds of kilometers, compared with the local scale of the tidal bore, there is several orders difference of magnitude. The tidal bore is usually simplified to be a strong discontinuity without thickness when we study the macro-scale problem. So the discontinuity-capturing method should be taken firstly when numerically simulating the tidal bore, which is required to choose high stability and resolution for the computational scheme, as well as the other requirements such as conservation of physical variables, accuracy, etc.

If the bottom topography and friction effect are negligible, the system of shallow-water equations is homogeneous, which is similar to Euler equation in aerodynamics, so a lot of standard shock-capturing methods that are well developed in aerodynamics can be applied to solve shallow water equations. Since 1980s, Zhao(1985), Xin(1991), Tan et al.(1995), Wang(1998), Su et al.(2001) have studied the numerical simulation of the tidal bore by using

these shock-capturing methods, and made a lot of progresses. All the work helps us understand more characteristic of this kind of flow phenomenon, the tidal bore.

However, bottom topography always exists, especially in the Qiantang Estuary, there is a large sand bar along the river, so the bed elevation varies greatly. Moreover, if bottom topography is negligible, it leads to "unbalanced solutions" that the stationary flow solution cannot be gotten even if the stationary initial condition and boundary condition are given (Xu, et al., 2002). Therefore the source term must be taken into account, especially the treatment of bottom topography, to keep the solutions balance.

When the shallow water equations with source term are solved with Godunov-type scheme, some new techniques are needed to keep the local Riemann problem hold, because the corresponding Riemann solution with source term is not available yet. Zhou, et al. (2001), Hui and Pan (2003) developed "Surface Gradient Method" and "Water Level-bottom topography Formulation (WLF)", respectively, which are all verified by the typical cases. In this paper, WLF Method is applied to numerically simulate Qiantang Bore, and further testing is performed compared with the observed tidal bore data in September 2000 (Lin, et al., 2002).

2. THE GOVERNING EQUATIONS AND THEIR SOLUTION

2.1 THE GOVERNING EQUATIONS

In order to simulate flows in complex plane-shaped domain, a transformation of coordinates is introduced from $(t,\ x,\ y)$ to $(t,\ \xi,\ \eta)$

$$\begin{cases} dt = d\lambda \\ dx = Ad\xi + Ld\eta \\ dy = Bd\xi + Md\eta \end{cases} \tag{1}$$

With the transformation (1), the arbitrary quadrilateral cells on $(t,\ x,\ y)$ can be transformed to rectangular cells on $(t,\ \xi,\ \eta)$. Here, A, B, L, M are calculated with geometric method. The unsteady 2-D shallow water equations can be transformed into the following conservative form:

$$\frac{\partial E}{\partial \lambda} + \frac{\partial F}{\partial \xi} + \frac{\partial G}{\partial \eta} = S \tag{2}$$

where

$$E = \begin{bmatrix} h\Delta \\ h\Delta u \\ h\Delta v \end{bmatrix} \qquad F = \begin{bmatrix} hI \\ hIu + \frac{1}{2}gh^2 M \\ hIv - \frac{1}{2}gh^2 L \end{bmatrix}$$

$$G = \begin{bmatrix} hJ \\ hJu - \frac{1}{2}gh^2 B \\ hJv + \frac{1}{2}gh^2 A \end{bmatrix} \qquad S = \begin{bmatrix} 0 \\ -gh\left(Mb_\xi - Bb_\eta + \Delta S_{fx}\right) \\ -gh\left(-Lb_\xi + Ab_\eta + \Delta S_{fy}\right) \end{bmatrix}$$

in which, u and v are x- and y-directions velocity components, respectively; h is water depth; g is acceleration due to gravity; b is bottom elevation; S_{fx}、S_{fy} are x- and y-directions friction forces, respectively; and

$$\Delta = AM - BL \qquad I = uM - vL \qquad J = vA - uB$$

It can be proven that the governing equation (2) is still hyperbolic (Hui et al., 2002).

2.2 OPERATOR SPLITTING AND GODUNOVE-TYPE SCHEME

In (ξ, η)-plane, the equation (2) can be discretized using finite volume method to

$$E_{i,j}^{n+1} = E_{i,j}^{n} - \frac{\Delta\lambda}{\Delta\xi_i}\left[F_{i+\frac{1}{2},j}^{n+\frac{1}{2}} - F_{i-\frac{1}{2},j}^{n+\frac{1}{2}}\right] - \frac{\Delta\lambda}{\Delta\eta_j}\left[G_{i,j+\frac{1}{2}}^{n+\frac{1}{2}} - G_{i,j-\frac{1}{2}}^{n+\frac{1}{2}}\right] + \Delta\lambda S_{ij} \qquad (3)$$

where the subscripts i and j represent the cell numbers in ξ- and η- directions, respectively; superscript n is the number of time step; $\Delta\xi$ and $\Delta\eta$ are ξ- and η-directions space step, $\Delta\xi_i = \xi_{i+\frac{1}{2}} - \xi_{i-\frac{1}{2}}$, $\Delta\eta_j = \eta_{j+\frac{1}{2}} - \eta_{j-\frac{1}{2}}$; $\Delta\lambda$ is time step; F and G are the numerical flux at ξ- and η-directions cell interfaces, respectively. In Godunov-type scheme, F and G may be constructed from the corresponding solutions of Riemann problem.

Using Strang splitting method, the 2-D problem is splitting into 2 1-D problems in ξ- and η- directions, then

$$E^{n+1} = R_{\frac{\Delta\lambda}{2}}^{\xi} R_{\Delta\lambda}^{\eta} R_{\frac{\Delta\lambda}{2}}^{\xi} E^{n} \qquad (4)$$

where, $R_{\Delta\lambda}^{\xi}$ and $R_{\Delta\lambda}^{\eta}$ are operators of 1-D equations in $\lambda-\xi$ plane and $\lambda-\eta$ plane, respectively. If $R_{\Delta\lambda}^{\xi}$ and $R_{\Delta\lambda}^{\eta}$ have second order accuracy in space, then equation (4) will have the same order in space.

If nonhomogeneous terms are removed, Riemann problem in $\lambda-\xi$ plain is simplified to

$$\begin{cases} \dfrac{\partial E}{\partial\lambda} + \dfrac{\partial F}{\partial\xi} = 0 & \lambda > 0 \\ E(0,\xi) = \begin{cases} E_l, & \xi < 0 \\ E_r, & \xi > 0 \end{cases} \end{cases} \qquad (5)$$

where

$$E = \begin{bmatrix} h\Delta \\ h\Delta\omega \end{bmatrix} \qquad F = \begin{bmatrix} h\omega \\ h\omega^2 + \dfrac{1}{2}gh^2 \end{bmatrix}$$

E_L and E_R are constant, ω is normal fluid velocity. Riemann problem in $\lambda-\eta$ plane is similar to that in $\lambda-\xi$ plane. The solution consists of at most four uniform flow regions, separated by three elementary waves: a shock (or expansion), a contact line, and expansion (or shock).

2.3 RIEMANN SOLUTIONS OF DRY BED

Riemann solutions of wet/dry bed can be given as following.

If dry bed is on right side,

$$E(0,\xi) = \begin{cases} E_L, & \xi < 0 \\ E_d, & \xi > 0 \end{cases}$$

in which, E_d denotes dry bed, then the solution of Riemann problem is

$$U_{Ld}(\lambda,\xi) = \begin{cases} U_L & if \quad \dfrac{\xi}{\lambda} \le \dfrac{S}{\Delta}(\omega_L - \sqrt{gh_L}) \\ U_{Lfan} & if \quad \dfrac{S}{\Delta}(\omega_L - \sqrt{gh_L}) < \dfrac{\xi}{\lambda} < s_{*L} \\ U_d & if \quad \dfrac{\xi}{\lambda} \ge s_{*L} \end{cases}$$

where

$$U = \begin{pmatrix} h & \omega \end{pmatrix}^T$$

$$s_{*L} = \frac{\mathrm{S_d}}{\Delta_d}(\omega_L - 2\sqrt{gh_L})$$

$$U_{Lfan} = \begin{cases} \omega = \omega_L + 2(\sqrt{gh_L} - \sqrt{gh}) \\ h = \dfrac{1}{9g}\left[\omega_L + 2\sqrt{gh_L} - \dfrac{\Delta}{S}\dfrac{\xi}{\lambda}\right]^2 \end{cases}$$

$$\Delta_d = \Delta_L$$

If dry bed is on left side, then

$$E(0,\xi) = \begin{cases} E_d, & \xi < 0 \\ E_R, & \xi > 0 \end{cases}$$

the solution of Riemann problem is

$$U_{Rd}(\lambda,\xi) = \begin{cases} U_d & if \quad \dfrac{\xi}{\lambda} \le s_{*R} \\ U_{Rfan} & if \quad s_{*R} < \dfrac{\xi}{\lambda} < \dfrac{\mathrm{S}}{\Delta}(\omega_R + \sqrt{gh_R}) \\ U_R & if \quad \dfrac{\xi}{\lambda} \ge \dfrac{\mathrm{S}}{\Delta}(\omega_R + \sqrt{gh_R}) \end{cases}$$

where

$$s_{*R} = \frac{\mathrm{S_d}}{\Delta_d}(\omega_R - 2\sqrt{gh_R})$$

$$U_{Rfan} = \begin{cases} \omega = \omega_R - 2(\sqrt{gh_R} - \sqrt{gh}) \\ h = \dfrac{1}{9g}\left[\omega_R - 2\sqrt{gh_R} - \dfrac{\Delta}{S}\dfrac{\xi}{\lambda}\right]^2 \end{cases}$$

$$\Delta_d = \Delta_R$$

The dry bed in the middle is not considered here, because this case will not happen in the natural river channel generally.

2.4 WATER LEVEL-BOTTOM TOPOGRAPHY FORMULATION

Because bed elevation is a function of x, and there are nonhomogeneous terms in its corresponding Riemann problem, it is difficult to get solution. Bed elevation is approximated by the average value of its adjacent cells, that is

$$\bar{b}_{i,i+1} = \frac{1}{2}(b_i + b_{i+1}) \qquad (6)$$

Then an approximate Riemann problem is formed, it also can be solved with the traditional method.

In order to guarantee the well-balanced computational results, bed slope term in equation (3) must be discretized in central difference method, and water depth of Riemnn solution is used, then the pressure term and bed slope term can be well balanced in both ξ and η directions.

3. NUMERICAL SIMULATION OF DAM BREAK WAVE

3.1 DAM BREAK WAVE ON NON-FLAT BED

The first example is about dam break problem on non-flat bed. Bed elevation is $b(x) = 1.398 - 0.347\tanh(8x - 4)$

And the initial conditions are:

$$\left(z_l = 1.0 + b(0),\quad u_l = 0.0\right)\Big|_{x<0.6} \qquad \left(z_r = 0.2 + b(1),\quad u_r = 0.0\right)\Big|_{x\geq 0.6}.$$

The results at t=0.08s are shown in Fig.1. It is clearly shown that the model in this paper has strong ability of shock-capturing.

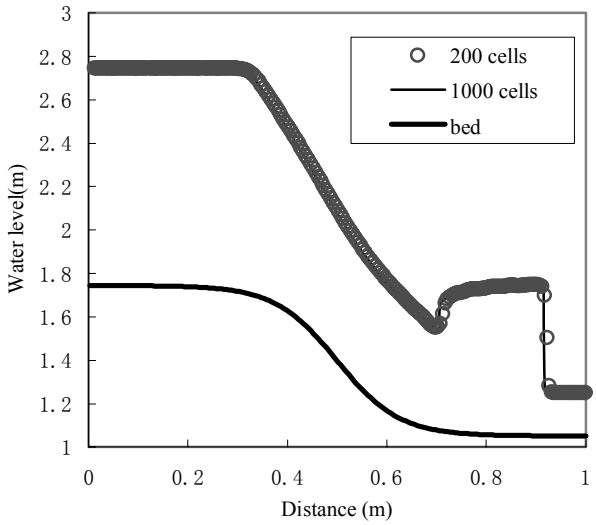

Fig. 1a Water level of dam break wave on non-flat bed

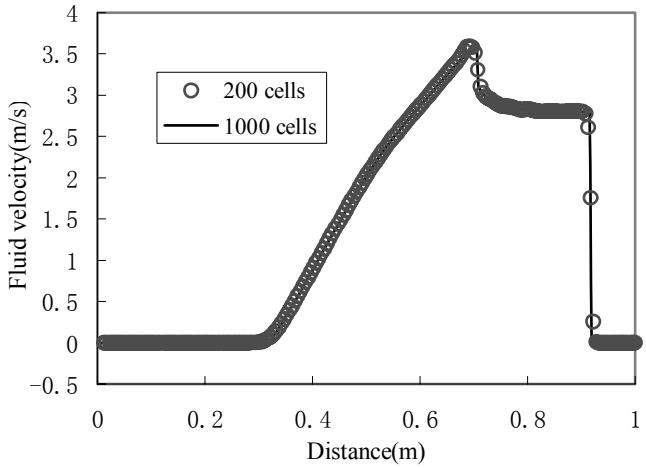

Fig. 1b Fluid velocity of dam break wave on non-flat bed

3.2 DAM BREAK WAVE ON DRY BED

The second example is dam break problem on dry bed. The computing domain is 0-100m, and the initial condition is

$$\left(z_l = 10,\quad u_l = 0.0\right)\Big|_{x<50} \qquad \left(z_r = 0,\quad u_r = 0.0\right)\Big|_{x\geq 50}$$

There are 200 computational cells, and time step is 0.01s. The comparison between the numerical solution and analytical solution at time t=2.5s is shown in Fig.2. A good agreement is made in water level between the numerical solution and the analytical solution. But there is much difference between computational velocity and the analytical one in the front of dam break wave. The reason is that the water depth is very small, but the fluid velocity is very large, so Fr number is more than 10,000. It is difficult to simulate this case, but the result is better than Vincent's(2001).

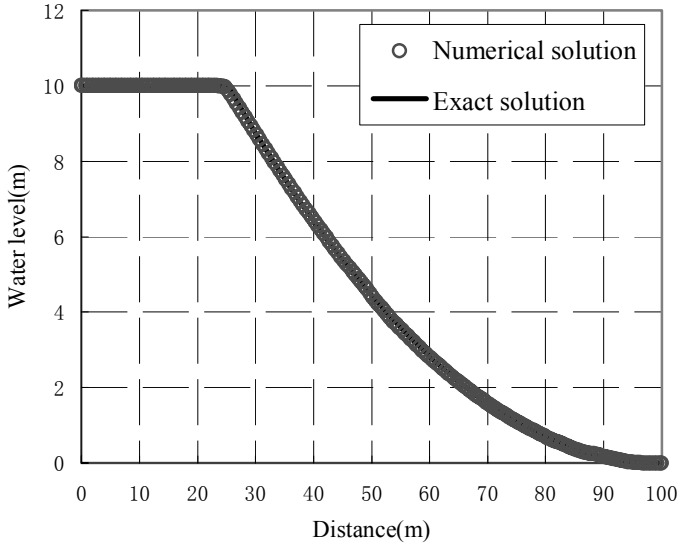

Fig. 2a Water level of dam break wave on dry bed

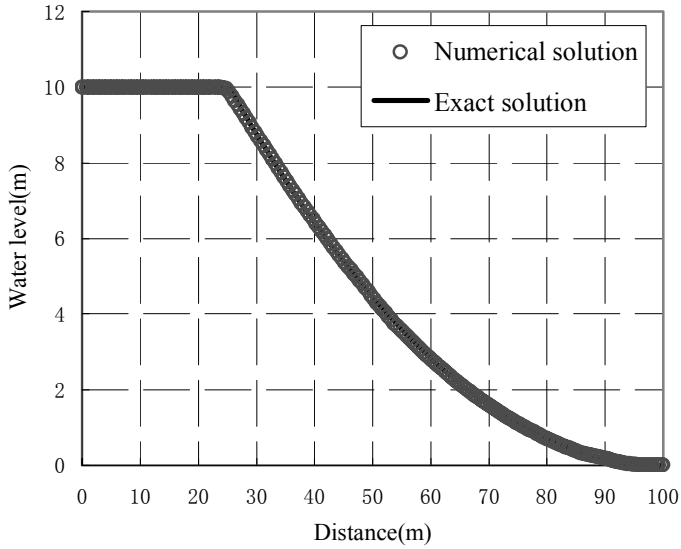

Fig. 2b Fluid velocity of dam break wave on dry bed

4. NUMERICAL SIMULATION OF QIANTANG BORE

The large-scale observation of tidal bore on the Qiantang River was organized in September 2000, from Hydraulic Power Station of Fuchun River to the cross-section of Jinshan in Hangzhou Bay, which includes runoff reach, estuary reach and part of current reach. Many tidal gauges were set up along the Qiantang River. The tidal level was observed continuously during half a month and was recorded at every 1–2 minutes when the tidal bore passes by the station. During the period of observation, typhoon "Sangmei" attacked the region, and it led autumn spring tide higher.The observed maximum tidal range is 7.72m at Ganpu.Based on the observation, more cognition about the propagation rule of Qiantang Bore can be gained, and it can provide the detail data for the study of numerical simulation. The verification of computational model is based on the data (Lin, et al., 2002).

4.1 COMPUTATIONAL CONDITIONS

A grid of 960×27 cells is laid over a region from Ganpu with 22km width to Changqian with 2km width over a distance of 72km, as shown in Fig. 3. The minimum distance of cell is 60m. Digital topography is generated using the map of July 2000. And the flow is computed

for three spring tides on 16-17 September 2000. The Manning coefficient is 0.004–0.005 for flood tide and 0.006–0.013 for ebb tide. Time step is 2s.

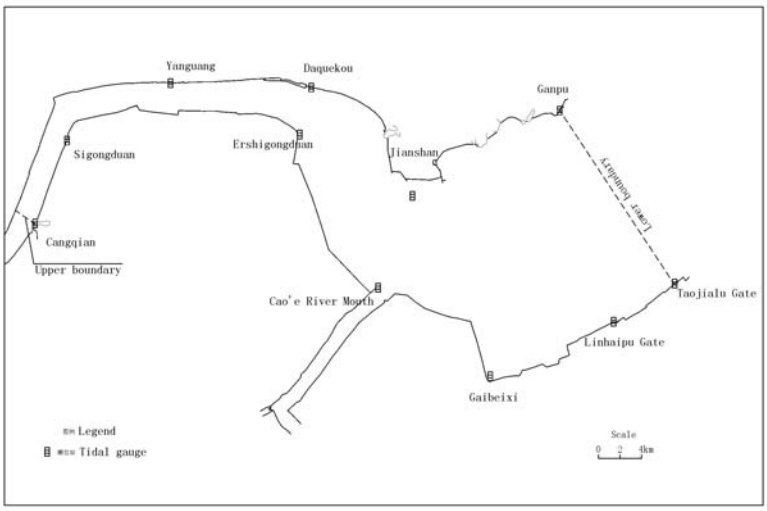

Fig. 3 Qiantang Estuary

4.2 BOUNDARY CONDITION TREATMENT

The normal velocity is set to zero on the solid-wall boundary. Using the theory of image reflection, a Riemann problem on solid-wall boundary can be solved, which may be done by employing a "ghost" cell outside the domain that is symmetric to the cell inside domain to construct a Riemann problem on solid-wall boundary.

The observed tidal level of the upstream and downstream water boundary is chosen as the boundary condition. The velocity of the corresponding point on the water boundary can be solved using 1-D characteristic difference method. There are much shoals in the Qiantang Estuary, so the moving boundary technique has much effect on the computational results. So Riemann problem in dry bed is constructed to do it.

4.3 COMPUTATIONAL RESULTS

There are seven tide gauges in the computational field. The hydrograph of computational result and observed data in Yanguan gauge can be seen in Fig.4, and the computational results show good agreements with the observed data.

The velocity is more than 3m/s in open boundary, Ganpu, where the observed velocity is available. The maximum computational velocity of flood tide and ebb tide as well as velocity process show excellent agreement with the observed data.

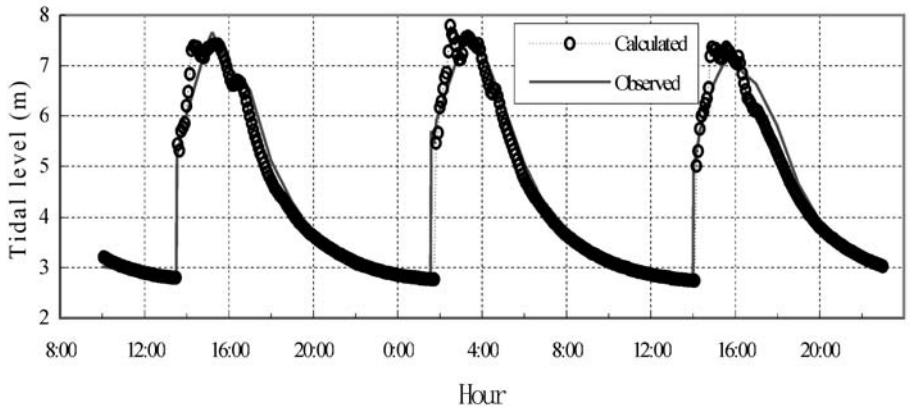

Fig. 4 Tidal level at Yanguan gauge

The computational results replicate the formation and development of the tidal bore. Table 1 shows water level changes at each tide gauge within a few minutes when the tidal bore passes by. Fig.5 is water surface profile along the channel at different moments. At the location downstream where the Cao'e River flows into the Qiantang River, water level jump of several centimeters height can be seen when flood tide front arrives. Here may be considered as the formation site of the tidal bore, then the height of the tidal bore increases gradually towards upstream. When the tidal bore gets to the Yan'guan station, the height of the bore reaches the highest one, of 1.83 meters increasing within one minute, then the bore height decreases gradually afterwards because of dissipation. It is shown that the tidal bore reaches the highest one at Daquekou station from the observed data. This is different from the computational result, and it may be caused by local topography approximation. During the observation, there is a mid shoal along Daquekou and a deep channel is near to the bank, so it is difficult to approximate the local topography in the model.

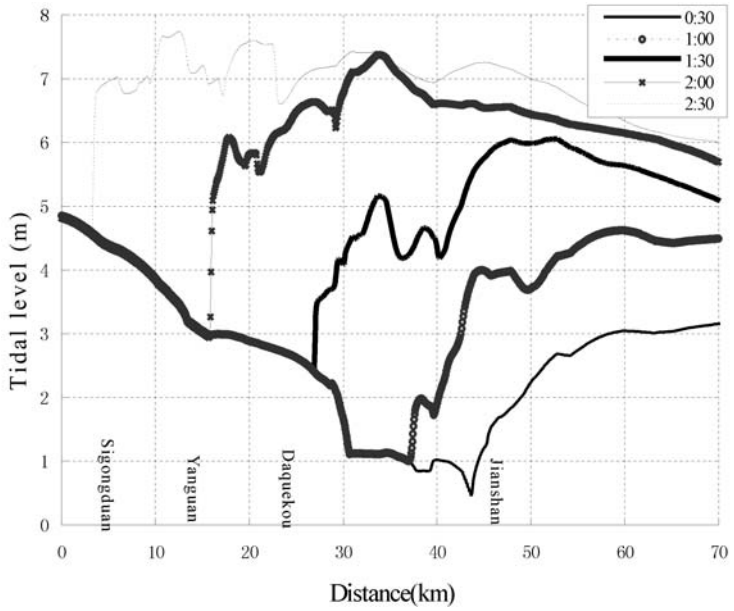

Fig. 5 Water surface profile along the channel at different moments

Table1 Tidal level and its changes in representative locations within five minutes after tidal bore arrival

unit: m

Time (minute)	Cangqian		Sigongduan		Yan'guan		Daquekou		At the mouth of Cao'e River	
	Tidal level	Change	Rise range	Change	Tidal level	Change	Tidal level	Change	Tidal level	Change
0	4.79		4.1		2.78		1.13		-0.41	
1	5.5	0.71	4.93	0.83	4.61	1.83	1.16	0.03	-0.37	0.04
2	6.34	1.55	5.36	1.26	4.78	2	1.83	0.7	-0.19	0.22
3	7.02	2.23	6.58	2.48	4.94	2.16	2.7	1.57	0.27	0.68
4	6.76	1.97	6.49	2.39	5.21	2.43	2.84	1.71	0.72	1.13
5	6.65	1.86	6.4	2.3	5.35	2.57	2.83	1.7	0.94	1.35
Observed change in 4–6		1.7		2.2		2.6		2.9		

Because the technical difficulties make it difficult to survey the data about the velocity around the tidal bore, the lack of the observed data leads us to know little about the characteristic of velocity round the tidal bore. We analyse the velocity along the river from

the computational result only. The velocity in time at the middle of Yan'guan's section is shown in Fig. 6.

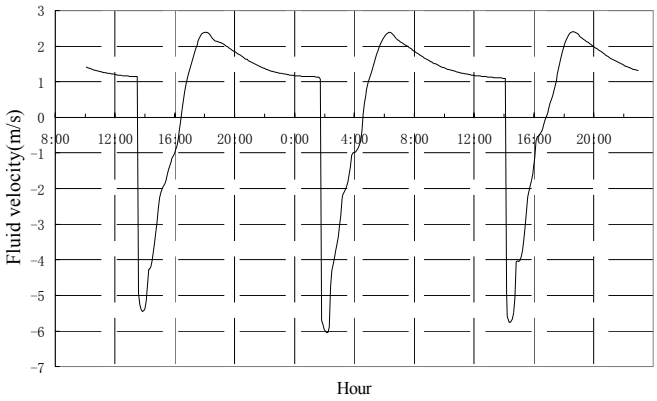

Fig. 6 Velocity in time at the middle of Yan'guan's section

According to the computational results, the contour of maximum velocity is plotted in Fig. 7. The maximum velocity in each place appears in the process of flood tide. Totally, the maximum velocity reaches 3–4m/s in the open boundary at Ganpu, then the velocity increases gradually upstream and gets the extreme one around Daquekou, where the velocity is more than 6m/s, then afterwards the velocity decreases a little. This process is in accordance with the height change of tidal bore.

As shown in Fig. 7, there is an area of high velocity, where the velocity is more than 7m/s, and the channel bends severely, for example, in Ershigongdaun and in the bank opposite to Laoyancang. The velocity reaches the highest one of 9.68m/s near Ershigongduan. This phenomenon is different from the others that high velocity happens in the concave bank of river channel. This phenomenon that the velocity in the convex side is much higher than in concave bank when the tidal bore passes has been verified in physical model.

From our numerical experiences, one of the great advantages of using Godunov-type scheme in the model is to simulate the high velocity flow successfully around the tidal bore. The maximum velocity reaches 9.68m/s in our computation. In history, the highest observed recorded of velocity is 12m/s, which provides more and less supports to our numerical results. And we think, that the vertical average velocity reaches 9–10m/s happens possibly in the strong tidal bore reach in the Qiantang river.

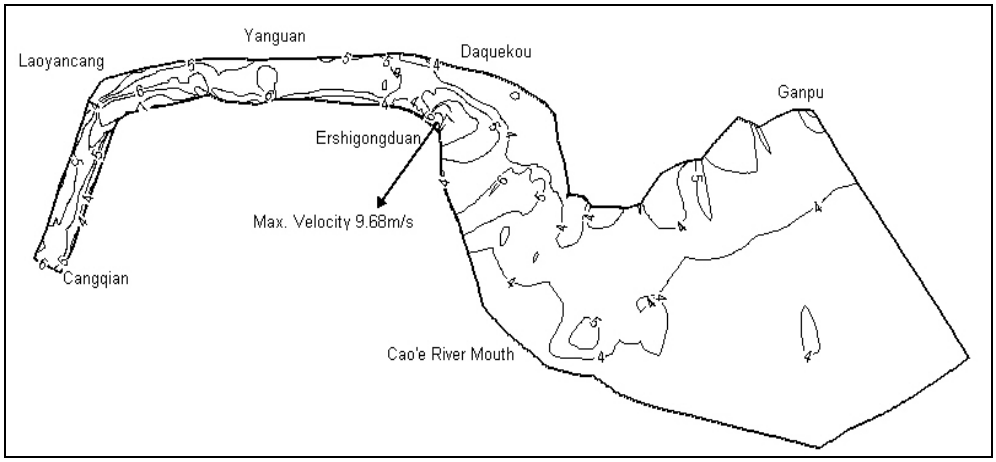

Fig. 7 The computational maximum velocity contour in Qiantang Estuary

According to our experiences, the flood velocity increases quickly and reaches the highest one after10-20 minutes. This is called as “high-velocity water” practically. This phenomenon is also seen in the computational results. Table 2 shows the sustaining time of the high velocity at different locations. From the table, “high-velocity water” appears in 9–40 minutes after tidal bore arrivals and it is not same at different locations. The tide somewhat possesses the characteristic of standing wave in the downstream Ganpu, the maximum flood velocity will appear in about 2 hours after the low tide. And it goes upstream, the maximum velocity appears earlier and earlier, for example, it only takes 9 minutes after the low tide around Sigongduan.

Table 2 High velocity and its sustaining time at representative locations

Place	high flood velocity(m/s)	Appearing time	Sustaining time of high velocity of more than 5.5m/s (minute)
At the mouth of Cao’e river	About 5	40 minutes after flood tide appears	0
Daquekou	>6	19 minutes after flood tide appears	8
Yanguan	>6	15 minutes after flood tide appear	33
Sigongduan	>6	9 minutes after flood tide appears	16

Sustaining time of high velocity has to relate to the maximum velocity. The sustaining time is more than half an hour at Yanguan location when velocity is more than 6m/s (Fig. 8).

During the propagation of tidal bore, some special horizontal patterns of the tidal bore appear, which are so called as “tidal bore sceneries”. The model replicates some of “tidal sceneries”. The tidal bore covers the cross-section around Yanguan, moving forward orderly, it is called as “a line-shaped tidal bore” (Fig.9). Then the tidal front curves gradually after passing by Yanguan. Bore reflections appear in many places when the tidal bore propagates and this phenomenon is called as “returning tidal bore”. “Returning tidal bore” is well known at the location of Laoyancang, where the bore reflects obviously and the difference of water levels between two banks may reach more than 3m, as seen in Fig.10. Fig.11 shows the intersections of tidal bores from Jianshan to Ershigongduan, which is called as “intersecting tidal bore”. So it is shown clearly that the model in this paper can simulate the macro-scale property of the tidal bore successfully.

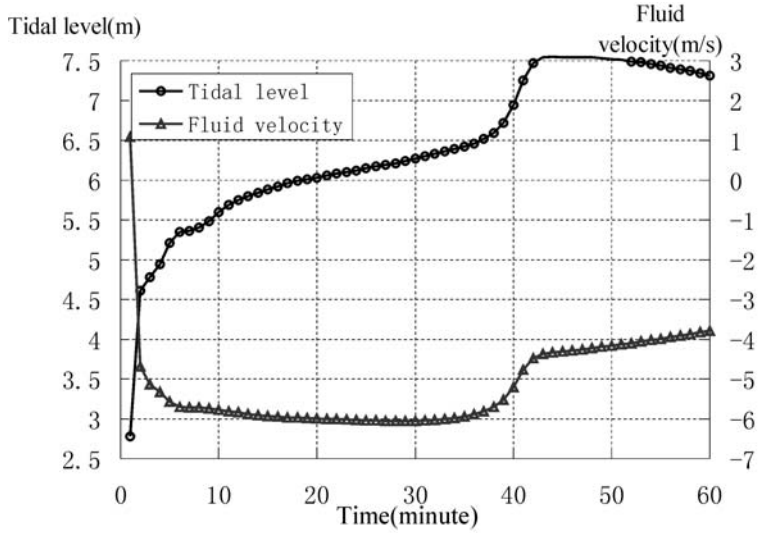

Fig. 8 The tidal level and velocity in one hour after tidal bore arrivals

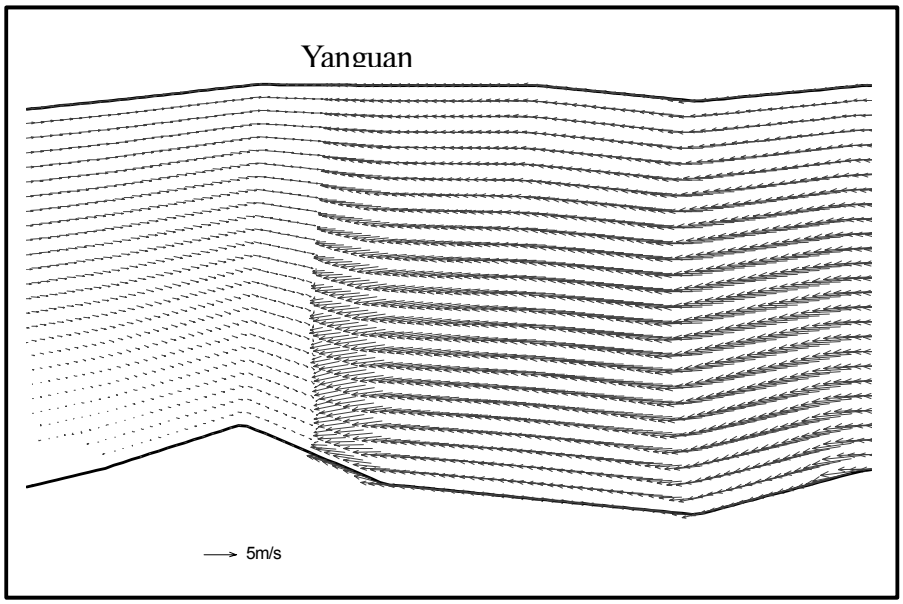

Fig. 9 Velocity at the moment when tidal bore appears in Yanguan reach

5. CONCLUSION

In this paper, the mathematical model is applied to simulate the formation, development, propagation, and dissipation of Qiantang Bore successfully by using Godunov-type scheme with WLF method. It can replicate the typical horizontal patterns of the intersecting, reflection of tidal bores and a line-shaped tidal bore in the processes of its propagation. Totally the model can simulate macro-scale properties of the tidal bore very well. From the experience, the progress in numerical simulation can lead more cognition of the tidal bore.

Because of the technical difficulties for survey, we know little about the characteristic of velocity near the tidal bore. Now combined with practical experience, the model provides detailed information for the study of tidal bore. In fact by this model, we have learnt more characteristic about the tidal bore.

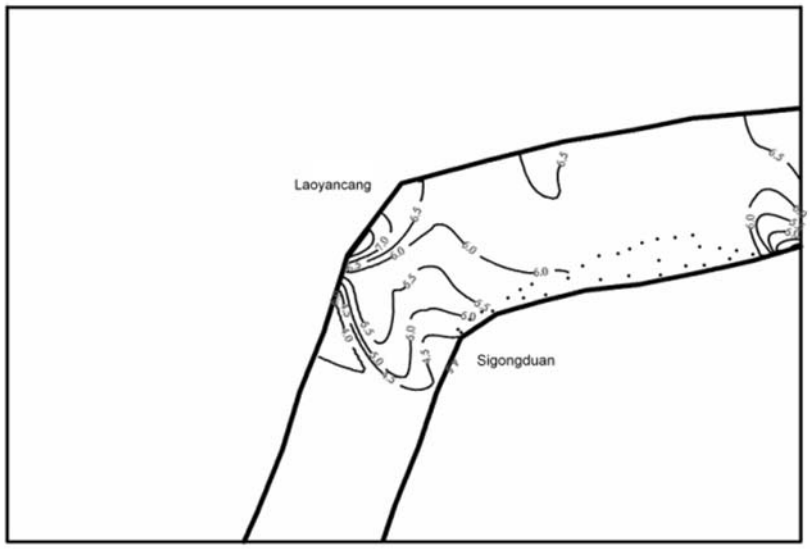

Fig. 10 Tidal level contour at the moment when tidal bore appears in Laoyancang reach

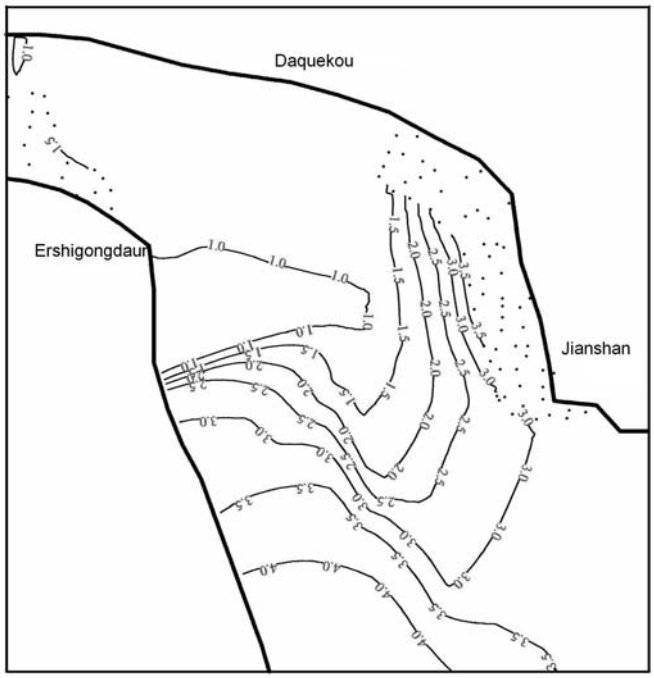

Fig. 11 Tidal level contour at the moment when tidal bore appears in Daquekou reach

ACKNOWLEDGEMENTS

Part of this work has been completed in the Mathematics Department of Hong Kong University of Science and Technology. Authors thank Prof. W.H.Hui in the department for his guidance and help.

REFERENCES

Hui WH, S Kudriakov, 2002. Computationa of the shallow water equations using the unified coordinates, *SIAM J Sci Comput*, Vol.23, pp.1615-1654.

Hui WH, Pan Cunhong, 2003. Water level-bottom topography formulation for the shallow-water flow with application to the tidal bores on the Qiantang river, *Computational Fluid Dynamics Journal (to be published)*.

Lin Bingyao, Huang Shichang, Mao Xianzhong, 1998. Analysis of undular hydraulic jump and undular bore, *Journal of hydrodynamics*, A, Vol. 13, No. 1, pp. 106-115.

Lin Bingyao, Huang Shichang, Mao Xianzhong, Pan Cunhong, 2002. Deformation process of tidal waves in Qiantang estuary. *Journal of hydrodynamics*, A, Vol.17, No.60, pp.665-675.

Marshall E. and Mendez R., 1981. Computational aspects of the random choice method for shallow water equations, *J. Comput. Phys.*, Vol.39, pp.1-21.

Pan Cunhong, Xu Xuezi，Lin Binyao, 1994. Simulation of Free Surface Flow near Engineering Structures Using MAC-Method, *Proceeding of the international Conference on Hydrodynamics,Wuxi*, China, pp.479-484.

Pan Cunhong, Lin Bingyao, Mao Xianzhong, 2003. A Godunove-type scheme for 2-D shallow-water flow with bottom toporgraphy, *Journal of hydrodynamics*, A, Vol.18, No.1, pp.16-23.

Su M.D., Xu X., Zhu J.L. et al, 2001. Numerical simulation of tidal bore in Hangzhou Gulf and Qiantangjiang, *Int. J. Numer. Meth. Fluids*, Vol.36, pp.205-247.

Tan Weiyan, Hu Siyi, Han Zengcui, Pan Cunhong et al., 1995. Two-Dimensional numerical modeling of bores in the Qiangtang estuary. *Advances in Water Science*, Vol.6, No.2, pp.83-93.

Tan Weiyan, 1998. Computational shallow hydrodynamics—Application of finite volume method[M], Beijing Tsinghua University Press.

Toro EF, 2001. Shock-capturing methods for free-surface shallow flows. Chichester: John Wiley & Sons.

Vincent S., Caltagirone J-P. and Bonnetion P., 2001. Numerical modeling of bore propagation and run-up on sloping beaches using a MacCormack TVD scheme, *Journal of Hydraulic Resear.*, Vol.39, No.1, pp.41-49.

Wan Dengcheng, 1996. The study of numerical method of vertical 2-D unsteady gravity flow with free surface, Scientific research report of Shanghai institute of application-mathematics and mechanics.

Wang Ruyun, 1998. Numerical imitating the generation and propagation of shallow-water bore. Dissertation for PhD degree of Oceanography Institute of Chinese Academy of Science.

Xin Xiaokang, 1991. Computation of 2-D tidal bore and pollution diffusing in Qiantang River. Scientific research report of the department of application-mechanics in Fudan University.

Xu Kun, Pan Cunhong, 2002. Kinetic flux vector scheme for the 1D shallow water equations with source terms. *Journal of hydrodynamics*, A, Vol.17, No.2, pp. 140-170.

Zhao Xuehua, 1985.1-D Mathematical Model of the tidal bore on the Qiantang River[J]. *Journal of Hydraulic Engineering*, No.1, pp.50-54.

Zhou J. G., Causon D. M., Mingham C. G. and Ingram D. M., 2001. The surface gradient method for the treatment of source terms in the shallow-water equations, *J. Comput. Phys.*, Vol.168, 1-25.